



This is a repository copy of *The effect of soil mineralogy and particle breakage on the impulse generated from shallow buried charges*.

White Rose Research Online URL for this paper:

<https://eprints.whiterose.ac.uk/199836/>

Version: Published Version

---

**Article:**

Lodge, T. [orcid.org/0000-0002-6906-0218](https://orcid.org/0000-0002-6906-0218), Clarke, S. [orcid.org/0000-0003-0305-0903](https://orcid.org/0000-0003-0305-0903), Waddoups, R. [orcid.org/0000-0002-2241-3784](https://orcid.org/0000-0002-2241-3784) et al. (3 more authors) (2023) The effect of soil mineralogy and particle breakage on the impulse generated from shallow buried charges. *Applied Sciences*, 13 (9). 5628. ISSN 2076-3417

<https://doi.org/10.3390/app13095628>

---

**Reuse**

This article is distributed under the terms of the Creative Commons Attribution (CC BY) licence. This licence allows you to distribute, remix, tweak, and build upon the work, even commercially, as long as you credit the authors for the original work. More information and the full terms of the licence here:

<https://creativecommons.org/licenses/>

**Takedown**



If you consider content in White Rose Research Online to be in breach of UK law, please notify us by emailing [eprints@whiterose.ac.uk](mailto:eprints@whiterose.ac.uk) including the URL of the record and the reason for the withdrawal request.



[eprints@whiterose.ac.uk](mailto:eprints@whiterose.ac.uk)  
<https://eprints.whiterose.ac.uk/>

## Article

# The Effect of Soil Mineralogy and Particle Breakage on the Impulse Generated from Shallow Buried Charges

Tommy Lodge <sup>1,2</sup>, Sam Clarke <sup>1,\*</sup>, Ross Waddoups <sup>1</sup>, Sam Rigby <sup>1</sup>, Matt Gant <sup>3</sup> and Ian Elgy <sup>3</sup><sup>1</sup> Department of Civil & Structural Engineering, University of Sheffield, Mappin Street, Sheffield S1 3JD, UK<sup>2</sup> Blastech Ltd., The Innovation Centre, 217 Portobello, Sheffield S1 4DP, UK<sup>3</sup> Defence Science and Technology Laboratory (Dstl), Porton Down, Salisbury SP4 0JQ, UK

\* Correspondence: sam.clarke@sheffield.ac.uk

**Featured Application:** Protection of vehicles and personnel from the devastating effects of landmines, shallow buried IEDs and explosive remnants of war remains a high priority in afflicted conflict and post-conflict areas. With most testing available in the literature having been conducted with quartz-based soils, this paper presents a comparative study on carbonate-based soils, as found in many regions across the world, providing data to allow the risk posed to vehicles and personnel to be assessed.

**Abstract:** Historically, most testing with shallow buried charges has focussed on soils which are predominantly quartz (silica)-based. Particle size, moisture content and density have previously been investigated to ascertain their importance, along with other geotechnical parameters, in governing the magnitude of an impulsive output. This has shown that, in order of importance, moisture content, density and particle size drive the total impulse imparted. The work in this paper presents the results of blast testing carried out with carbonate sands to investigate the difference that particle mineralogy (and hence, propensity for breakage) has on both the localised loading and the total impulse using an array of 17 Hopkinson pressure bars known as the Characterisation of Blast Loading (CoBL) apparatus. Carbonate sands are thought to have more friable particles due to their plate-like morphology, as opposed to the rounded morphology of quartz-based sands. Testing was conducted with low moisture content samples and compared with the well-established Leighton Buzzard uniform sand to isolate the effect of particle mineralogy/morphology on the loadings measured. The results show that, despite attaining a 23% lower bulk density, carbonate soils deliver almost identical total impulses (0.7–3.0% higher) when compared with quartz soils for nominally identical moisture contents.

**Keywords:** buriedcharges; landmines; soils; carbonate; total impulse



**Citation:** Lodge, T.; Clarke, S.; Waddoups, R.; Rigby, S.; Gant, M.; Elgy, I. The Effect of Soil Mineralogy and Particle Breakage on the Impulse Generated from Shallow Buried Charges. *Appl. Sci.* **2023**, *13*, 5628. <https://doi.org/10.3390/app13095628>

Academic Editors: Ricardo Castedo and Syed Minhaj Saleem Kazmi

Received: 13 January 2023

Revised: 29 March 2023

Accepted: 26 April 2023

Published: 3 May 2023



**Copyright:** © 2023 by the authors. Licensee MDPI, Basel, Switzerland. This article is an open access article distributed under the terms and conditions of the Creative Commons Attribution (CC BY) license (<https://creativecommons.org/licenses/by/4.0/>).

## 1. Introduction

There is a wealth of research and activity across the world to combat the threat posed by landmines. Globally, there are over 10,000 casualties caused by landmines, explosive remnants of war and improvised explosive devices each year [1], highlighting how there is still an ongoing need for research in this area. Through the improved understanding gained by this work, better predictive models can be produced to assist in the development of protective systems e.g., demining suits, potentially saving thousands of lives globally. In the context of this work, a buried charge is an explosive surrounded by soil and is of interest due to its potential to cause significant harm to a vehicle or person when detonated. Westine et al. [2] proposed that, in the case of a buried charge, the loading is primarily impulsive due to the material striking the target rather than being due to shock wave loading. This was further verified by others, including Ehr Gott et al. [3] who measured both the air shock and the impulse transferred to a rigid target. They found that the air pressure

measurements alone were not able to predict the total impulse, including the contribution due to soil throw. Therefore, an understanding of the soil mechanics is vital.

The Westine model [2] allows for a first-order approximation of the impulse from a buried charge to be calculated; however, the soil is categorised solely on its bulk density. More recent work has investigated additional parameters, including moisture content [4–8], void ratio and permeability [3,7,9,10], particle size distribution [3,7,11,12] and soil mineralogy (quartz [3,7,8,12], clays [3,4,7] and alluvial soils [8,12]).

In the parameters identified above, there are interdependencies between the different variables; for example, moisture content, air void ratio and permeability are all related to the ratio of air, water and solid particles in the sample. In soil mineralogy studies, the chosen samples vary both in their mineralogy and in their particle size and cohesion, e.g., clay and alluvial soils are highly cohesive when compared with quartz-based sands. When reporting the geotechnical conditions of a burial, researchers typically focus on the properties which are commonly measured such as particle size, moisture content and density. These parameters have been previously shown to govern the impulsive output of explosive charges buried in soils. It has been shown that, in order of importance, moisture content, density, and particle size drive the total impulse delivered. However, particle size does have a dramatic impact on the localised loading delivered to a target, especially where larger gravel-size particles are included.

Quartz (silica)-based sands make up the majority of sands in on-shore non-tropical regions. Hence, they have been the primary focus of research when looking at the effect that soil has on the output from a buried charge. The second most prevalent sand worldwide is calcium carbonate, referred to in this paper simply as carbonate sands, which are important where littoral conditions are encountered. Carbonate sands are found where coral reefs have historically been formed and tend to vary dramatically from quartz sands in the shape of their particles, their intraparticle voids and their susceptibility to breakage [13,14].

This paper presents an experimental investigation into the influence of soil mineralogy on the loading arising from the detonation of shallow-buried plastic explosives (PE4), with a focus on carbonate sands. We aim to show the effect that particle mineralogy has on both the localised loading and total impulse for a single stand-off distance. One characteristic of carbonate sands is that their particles are inherently more friable due to their plate-like morphology [15,16]. To isolate the effects of particle mineralogy, testing was conducted on prepared soil samples with low moisture contents to enable a direct comparison with the historic dataset on soils from testing at the University of Sheffield [17]. The secondary aim of this paper is to identify whether particle breakage can have an effect on both the magnitude and distribution of loading from shallow buried charges. Much work has gone into quantifying the degree of particle breakage from single-diameter measures to area-based breakage indices [18]. More recently, the potential for breakage has been informed by fractal (ultimate) grading, e.g., refs. [13,19,20]; the reader is referred to the work of Yu for a recent overview of this topic [21]. Differences in particle shape are also known to affect other mechanical properties of soil [22–24]. These behaviours are established at stresses <1 MPa, but due to the limit of such theories in high-stress (>100 MPa) blast regimes, the consideration of such factors are outside the scope of this paper.

## 2. Materials and Methods

### 2.1. Test Apparatus

The Characterisation of Blast Loading (CoBL) apparatus is housed at the University of Sheffield's explosive test laboratory in Buxton, UK. It was designed and constructed in 2013 to measure the spatial and temporal distribution of a loading due to a shallow-buried charge and has been widely reported [17,25,26]. The CoBL apparatus, shown diagrammatically in Figure 1, consists of 17 Hopkinson pressure bars (3.25 m long and 10 mm diameter EN24(T) steel) suspended from the top, with the bottom face flush with the surface of a rigid target plate. The bars are suspended from the distal end such that their faces sit flush with (and are uncoupled from) the loaded face of the target. The apparatus allows the arrangement

of the bars to be varied depending on the tests being undertaken; for this work, they were arranged as two perpendicular lines of 8 bars with a shared central bar. The distance between each pair of bars is 25 mm (centre-to-centre). The spatial and temporal pressure histories are obtained by analysing the Hopkinson bar signals, enabling measurement of the specific impulses at discrete locations across the target face and calculation of the total area-integrated impulse over the instrumented region (200 mm diameter).

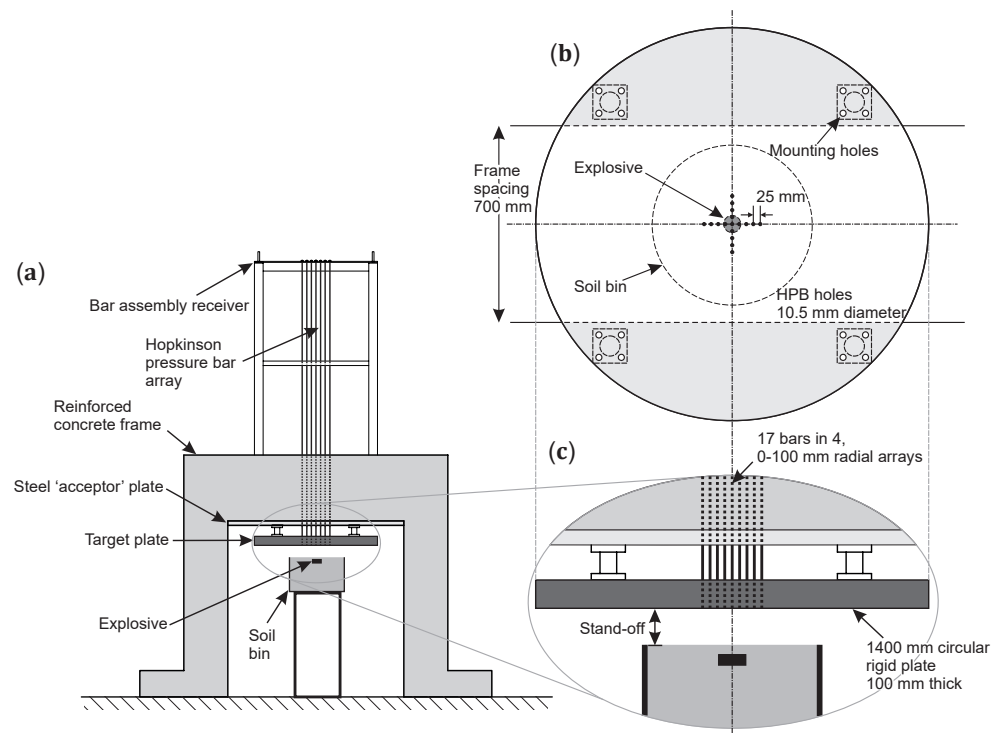


**Figure 1.** (a) Diagrammatic representation of the CoBL apparatus showing the soil container, target plate, and array of Hopkinson pressure bars. (b) Plan view of the target plate showing the arrangement of the bars in relation to the explosive charge and soil container. (c) Detailed view of the target plate. Adapted from [27].

## 2.2. Explosive and Burial Conditions

Testing was conducted with 78 g PE4 charges formed into 3:1 diameter/height cylinders. This is a quarter-scale equivalent of 5 kg PE4 (6 kg TNT equivalence [28]). The charges were buried at a depth of 25 mm (100 mm full-scale equivalent) but with an additional 3 mm of soil overburden provided to account for the removal of the lid of the 3 mm thick PVC casing, which was found to interfere with repeatability during preliminary testing [29]. The stand-off distance from the soil surface to the target was set at 140 mm. These conditions are the same as in previously reported work [17] to allow for a direct comparison and are contained within Table 1.

**Table 1.** Summary of experimental parameters held constant.

Parameter	Value	Units
Burial depth <sup>1</sup>	28	mm
Stand-off distance (Figure 1c)	140	mm
Charge radius	30	mm
Charge thickness	20	mm
Explosive type	PE4	-
Charge mass	78	g

<sup>1</sup> Defined as the depth of soil above the top surface of the charge.

### 2.3. Soil Details and Predictions

To investigate the effect of soil particle mineralogy, carbonate sand was chosen as it is predominantly made up of plate-like particles, in stark contrast to the more spherical quartz-based sands tested previously [17,25–27]. Figure 2 shows electron microscopy of the two sands used in this work at different levels of magnification. Previous work [7] conducted testing on three sizes of quartz-based Leighton Buzzard (LB) sand. The three sizes used were LB Fraction B (hereafter referred to as LB); 2LB, which is approximately double the size of LB Fraction B; and LBF, which is a better graded sand sized between LB and 2LB. Clarke et al. [7] found that small changes in particle size within this range did not result in differences in total impulse; therefore, any changes in loading observed in the current work with sand of similar sizes can be attributed to other factors.

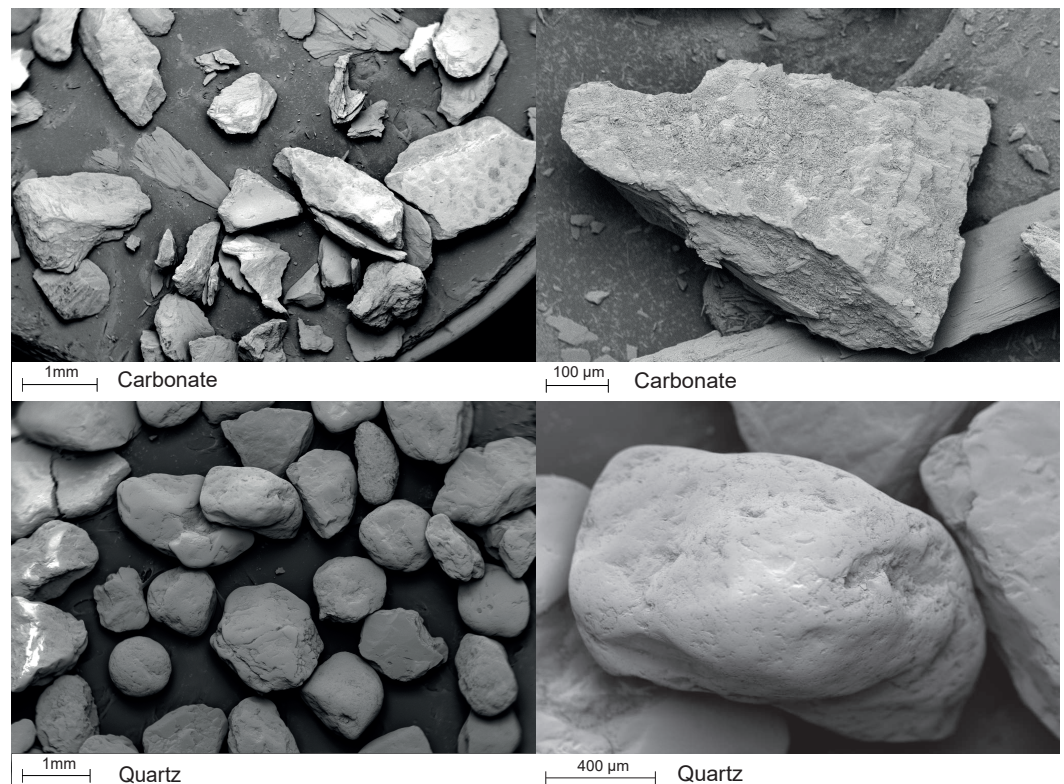


**Figure 2.** Electron microscope images of the two types of sand tested: the left-hand images show the difference in particle shapes and the right-hand images show the difference in surface texture of the particles.

In this study, we define carbonate sand as having greater than 50% calcium carbonate content. Soils with less than 50% calcium carbonate are known as calcareous soils. Due to the large quantities of sand required for blast testing, a sustainable source of sand of the correct particle size distribution (and mineralogy) was required. The material used was aquarium sand manufactured from sea washed shells (calcium carbonate) produced by Tropical Marine Centre. Tropical Marine Centre’s ‘EcoSand Fine’ was found to be the most suitable as it has a particle size distribution between fractions of Leighton Buzzard sand used in previous testing that were shown not to have a notable effect on impulse [7]. The bulk density of the carbonate sand was measured to be  $1.27 \text{ Mg/m}^3$  ( $w = 5\%$ ), which is considerably lower than the density of  $1.67 \text{ Mg/m}^3$  ( $w = 5\%$ ) measured for LB ( $G_s = 2.65$ ,  $\rho_{dmin} = 1.48 \text{ Mg/m}^3$ ,  $\rho_{dmax} = 1.74 \text{ Mg/m}^3$  and  $D_r = 73\%$ ). It is well known that the intraparticle voids play a large role in the reduced bulk densities seen in carbonate sands, leading to an expected range of  $1.15\text{--}1.5 \text{ Mg/m}^3$  [16]. The minimum and maximum densities were  $1.04$  and  $1.31 \text{ Mg/m}^3$ , respectively, giving a relative density  $D_r = 85\%$ . The specific gravity is  $2.73$ , being slightly higher than that for LB.

It has been shown in previous work that increasing bulk density led to an increased measured impulse but that moisture content had a greater effect increasing impulse than the added mass alone would suggest [11]. This led to the development of a modification to the Westine model [2] to determine the loading from a buried charge [7]. The Westine model quantifies the soil based on its bulk density alone, whereas the Clarke et al. [7] model extends this to include moisture content. Equation (1) gives the formulation of the Clarke et al. model, which determines the impulse relative to the baseline condition of dry (0% moisture content) quartz sand at a bulk density of  $1.6 \text{ Mg/m}^3$ . In previous work, a lower bound of  $1.6 \text{ Mg/m}^3$  for moisture content was deemed acceptable due to the minimum densities achievable in silica-based soils.

$$I_{mod} = 0.9 - 0.096w + 0.033\rho + 0.078w\rho \quad (1)$$

where  $w$  is the gravimetric moisture content (%) and  $\rho$  is the soil bulk density ( $\text{Mg/m}^3$ ). Equation (1) has been rounded to 2 significant figures here as the extra precision makes no practical difference to predictions.

This model predicts that, for two soils with the same moisture content and comparable particle size distribution to the baseline, the one with a higher bulk density will result in a larger loading. In addition, it predicts that, for soils with a bulk density above  $1.23 \text{ Mg/m}^3$ , increasing the moisture content also increases the loading. Below this density, the empirical nature of the model means the outputs are non-physical.

Figure 3 shows the expected increase in loading compared with the baseline used in the Clarke et al. model. For the carbonate sand density achieved in the current work, testing at 2.5% moisture content with all other factors consistent, an 8.4% reduction in loading compared with dry quartz sand would be expected. Any variation in impulse measured from carbonate sands is likely caused by other geotechnical factors not included in the original  $I_{mod}$  formulation.

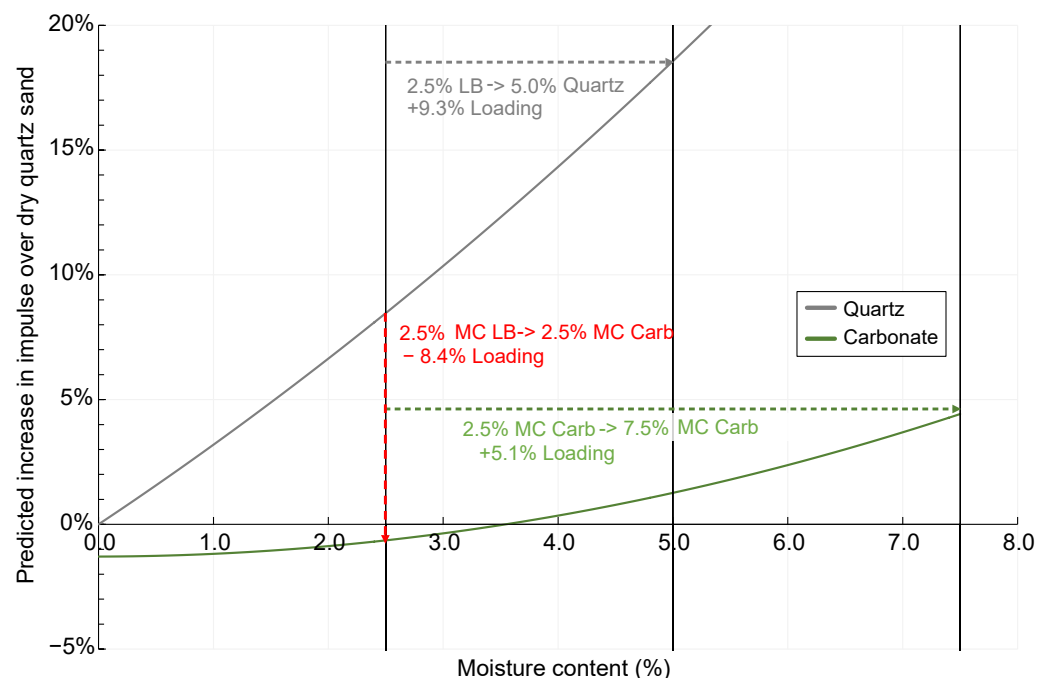


**Figure 3.** Plot showing the application of the moisture content prediction of Clarke et al. [7] to the two soil types considered in this paper.

#### 2.4. Sample Preparation

Prior to testing, soil samples are prepared to the desired geotechnical conditions in steel soil containers in accordance with the previously reported technique [30]:

1. Baseline soil moisture content of the as-delivered sand is measured.
2. Water is added to achieve the desired moisture content.
3. Soil is mixed thoroughly using a paddle action mixer.
4. Half of the soil is added to the container and compacted to the desired density.
5. The remaining soil is added and compacted to the desired density.
6. Any extra soil above the surface of the container is screeded off to leave the surface flat.
7. A waterproof membrane is attached to seal the container and to prevent any moisture loss prior to testing.

Immediately prior to testing, the following occur:

8. A void is excavated in the centre of the soil with the removed material saved.
9. The charge is placed in the void at the desired depth.
10. Removed material is used to backfill the hole to the desired density.

This procedure was developed for previous work, which demonstrated that with tightly controlled soil conditions, the variation in loading is significantly reduced, with 80% of the reported data lying within  $\pm 3.7\%$  of the mean for a given test series [11]. This is lower than that achieved with the standard “Minepot” tests defined in AEP-55 [31].

### 2.5. Analysis Process

Measured pressure traces were temporally integrated over the period of the loading to determine the specific impulse measured at the given bar location. Bars at the same radial offset for each test series were then combined to produce an average for that distance. This approach aims to reduce the skew of any localised increases in loading due to jets and instabilities present in the loading histories, seen also in similar free-air studies [32].

The specific impulse at the 17 discrete measurement locations were then integrated with respect to area to give a value for the total impulse within the 100 mm instrumented region. This total impulse can then be used as a single metric to facilitate comparison between different test series.

## 3. Results

### 3.1. Figures, Tables and Schemes

Table 2 summarises the new experiments performed and historic data analysed in this paper. In total, 12 tests were conducted on carbonate sands, yielding 204 pressure–time traces, which were combined with data from 7 historic tests (a further 102 traces).

**Table 2.** Summary of data used in this analysis.

Series Name <sup>1</sup>	Bulk Density (Mg/m <sup>3</sup> )	Measured Moisture Content (%)	Number of Tests
Carbonate sand 2.5%	1.259	2.31	3 repeats
Carbonate sand 5.0%	1.265	4.76	3 repeats
Carbonate sand 7.5%	1.305	7.49	3 repeats
Quartz (LB) sand 2.5%	1.635	2.45	4 repeats [17]
Quartz (LB) sand 5.0%	1.670	4.76	3 repeats [17]

<sup>1</sup> Series name denotes soil type and target moisture content for testing.

### 3.2. Pressure Data

Figure 4 shows a typical pressure trace recorded from the Hopkinson bars. The five signals correspond to the data from one of the radial lines and the central bar. The varying arrival times for the signals demonstrate how the loading reaches the central region first and then spreads out over the target plate. As is to be expected, the delay between the central bar and the 25 mm bar is small as the charge extends radially to the 25 mm bars (as shown Figure 1b). The shape of the pressure pulse approximately resembles that of an explosive air shock, which is in agreement with previous work on dry sand [33].

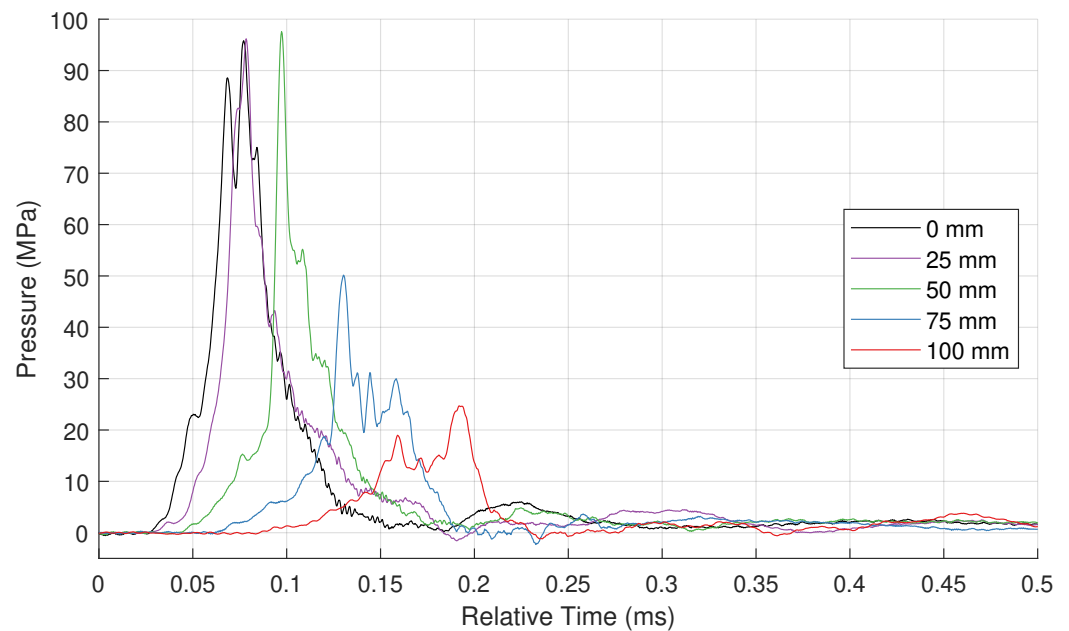


**Figure 4.** Pressure time history for five bars in a single test (other traces excluded for clarity).

### 3.3. Particle Size Distribution

To quantify the degree of particle breakage, samples from before and after testing were initially evaluated with a laser diffraction particle size analyser (Malvern Mastersizer 3000) to determine the particle size distribution (PSD). It was found that the small sample size (approximately 5 g) required for the laser diffraction analysis was very sensitive to small quantities of dust and soot in the post-blast test samples, and therefore, a sieve analysis was conducted using larger samples (>100 g) to rule out any sampling errors. The results of the PSD analysis are presented in Figure 5, which shows that there is a larger degree of particle breakage in the quartz-based sand than the carbonate sand. This is further apparent when comparing the  $D_{10}$ ,  $D_{50}$ ,  $C_c$ , and  $B_t$  factors (summarised in Table 3), which are the sizes above which 10% and 50% of the measured diameters fall, and the total breakage factor defined by Hardin [18], respectively. The total breakage factor ( $B_t$ ) represents the change in the integral of the particle size distribution curve and measures the degree of overall particle breakage in the sample:

$$B_t = \int_0^1 (b_{p0} - b_{pl}) df \quad (2)$$

in which  $b_{p0}$  = the original values of  $b_p$ , and  $b_{pl}$  = the values of  $b_p$  after loading.  $b_p$  is the potential for breakage of a particle of a given size,  $D$ , and may be represented by

$$b_p = \log_{10} \left[ \frac{D \text{ in mm}}{0.074 \text{ mm}} \right] \text{ for } D \geq 0.074 \text{ mm} \quad \& \quad b_p = 0 \text{ for } D < 0.074 \text{ mm} \quad (3)$$

The quartz sand samples consistently show a higher degree of breakage than the carbonate sand; however, the overall change is still small (e.g., a 3.3% reduction in the median particle size and breakage factor of 7.4% for quartz sand). Figure 5 and Table 3 show that there is no substantial increase in particle breakage for the carbonate sand; in fact, the results show a lower degree of breakage than that in the quartz sand contrary to previous findings [15]. The lack of substantial difference in breakage of the carbonate sand would therefore predict that the loading follows the trend outlined in Figure 3 and Equation (1).



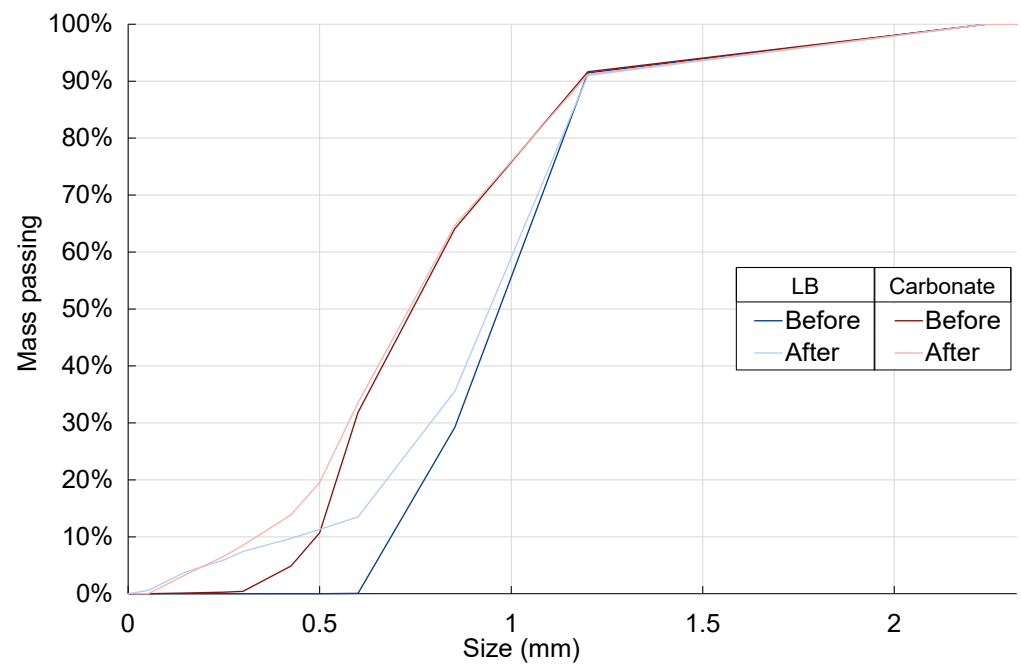


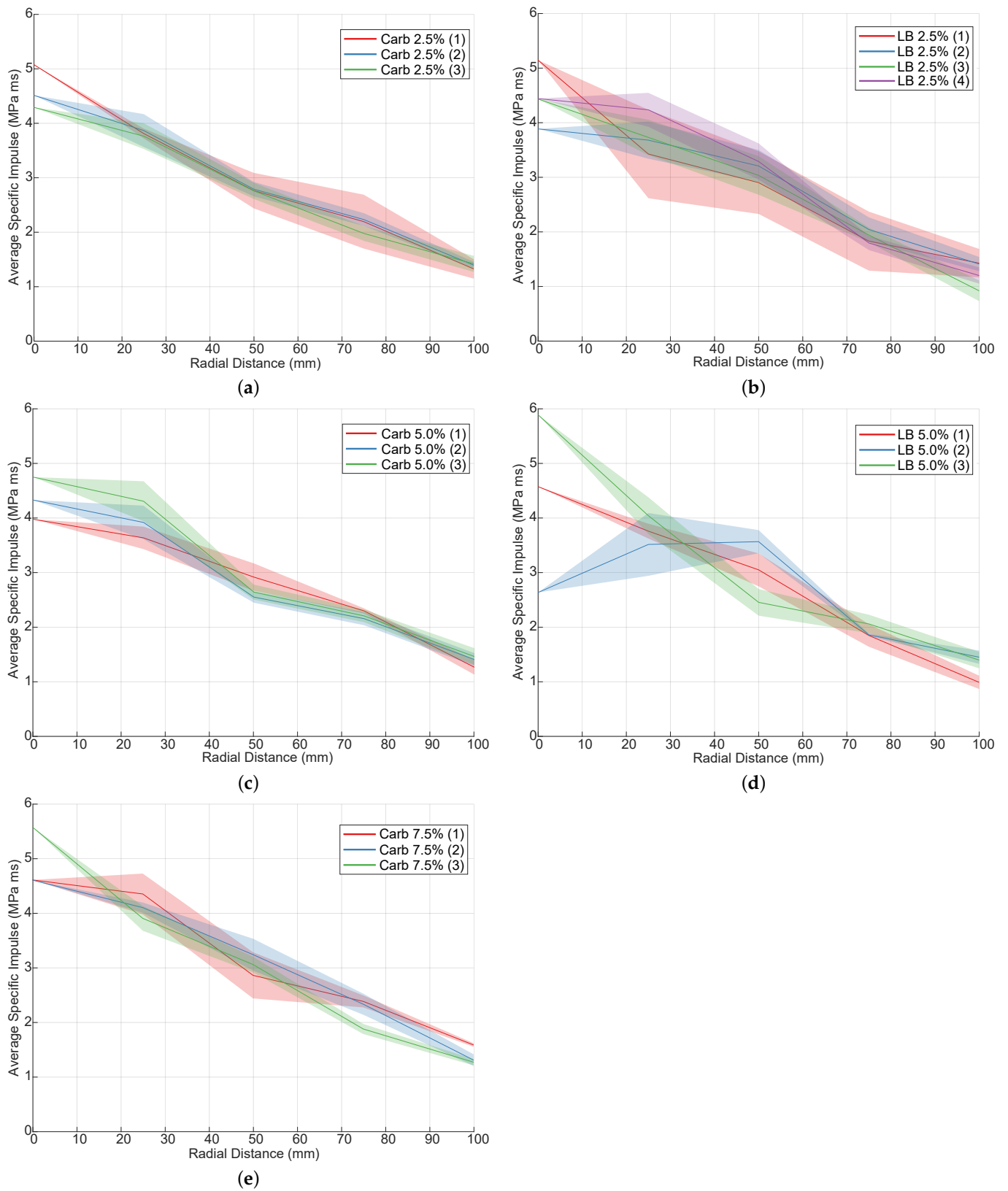
**Figure 5.** Particle size distribution of quartz (LB) and carbonate sand before and after blast testing using sieve analysis.

**Table 3.** Summary of particle size distribution parameters for both soil types before and after testing, all values in mm unless otherwise specified.

Sand	Pre			Post			$B_t$
	$D_{10}$	$D_{50}$	$C_u$	$D_{10}$	$D_{50}$	$C_u$	Total Breakage
Quartz	0.686	0.970	1.494	0.440	0.938	2.264	7.3%
Carbonate	0.491	0.742	1.672	0.335	0.734	2.433	4.2%

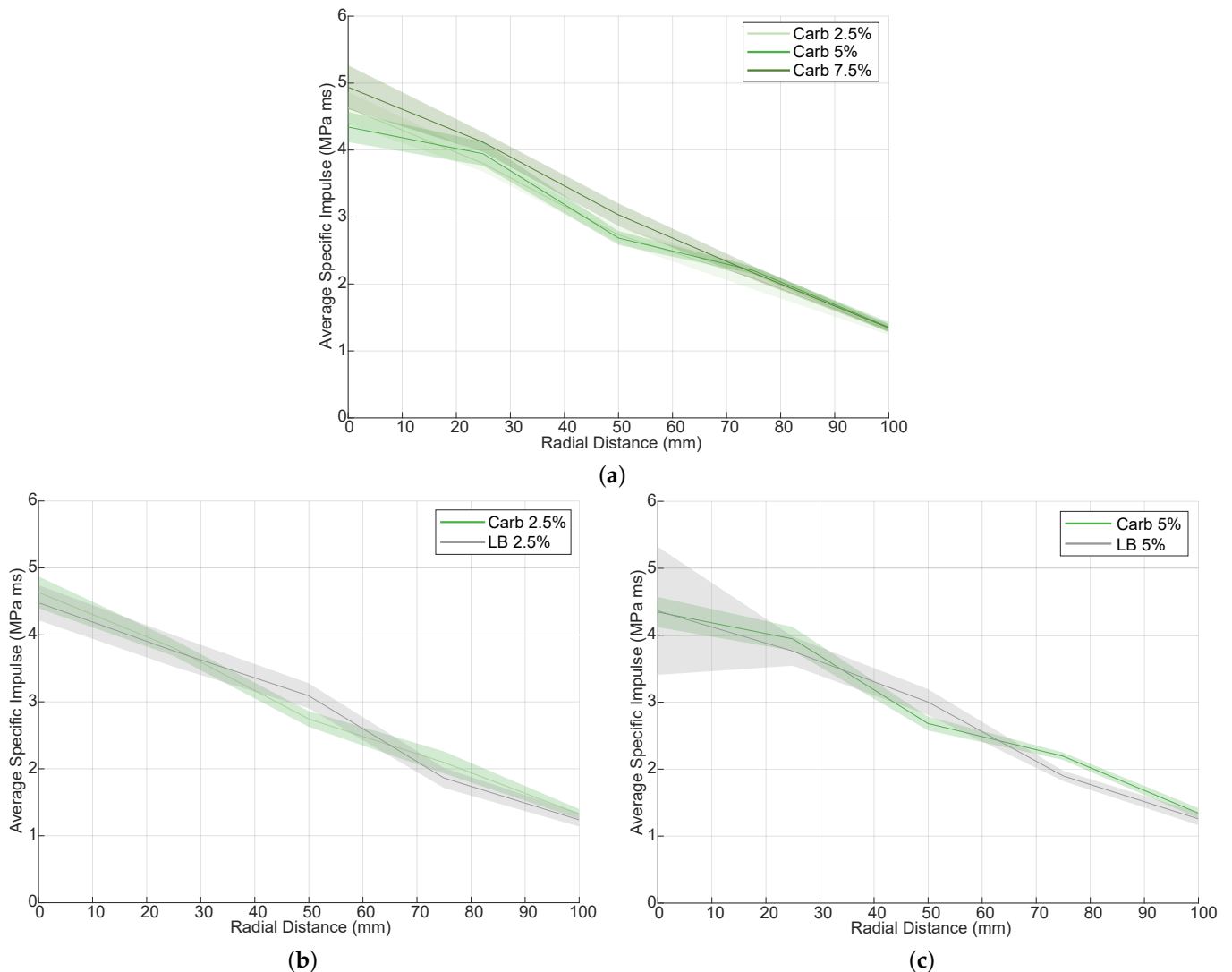
### 3.4. Specific Impulse Distribution

Figure 6 plots the average specific impulse for each test in each series as a function of radial distance. The shaded region indicates the standard error on the mean within a given test (based on the four measurements for each radius and one for the central bar). It can be seen that there is a good test to test the consistency for measurements at radii of 25 mm and above. The variation in the loading at the central measurement point is to be expected as there is a single measurement point that is highly sensitive to small variations in the charge position. Figure 6a,c,e show the effect of increasing moisture content on the pressure distributions. As expected, at low moisture contents, there is no phenomenological difference in the distributions and the increase in total impulse (from the integrated signals discussed later) shows a minimal increase with increasing moisture content. Figure 6a,b show the specific impulse distributions for the carbonate and LB tests at the same moisture contents. LB has historically been identified as a soil which generated very repeatable loading [11] (especially in comparison with well-graded soils). The carbonate test results show a tighter spread on impulse distributions, thus making this an exceptionally repeatable test condition. The impact of this will be discussed later in the total impulse calculations.



**Figure 6.** Specific impulse distribution for the five series considered; each plot shows the results for the repeat tests within the given series and demonstrates the repeatability of the data. (a) Carbonate at 2.5% moisture content; (b) quartz at 2.5% moisture content; (c) carbonate at 5.0% moisture content; (d) quartz at 5.0% moisture content; (e) carbonate at 7.5% moisture content.

Figure 7 plots the specific impulse as a function of radial distance averaged across all measurement points in a given series (i.e., the average of the results from multiple measurement points in all the nominally identical tests shown in Figure 6). It can be seen in Figure 7a that, as the moisture content of the carbonate sand increases, there is a small increase in the measured loading. This is in agreement with the results of Clarke et al. [17], who investigated the effects of moisture content in quartz-based sands. Figure 7b,c show that both the magnitude and spatial distribution of the loading for carbonate and quartz sand is comparable and, again, highlights the level of repeatability achievable with careful control over the soil preparation.



**Figure 7.** Specific impulse distributions comparing the sand types at varying moisture contents. (a) Carbonate sand at 2.5%, 5.0% and 7.5% moisture contents; (b) quartz and carbonate sand at 2.5% moisture content; (c) quartz and carbonate sand at 5% moisture content.

### 3.5. Total Impulse

Figure 8 shows the total interpolated impulse over the 100 mm radius instrumented region for each test, along with the average value for each series. It can be seen that, as the moisture content of the carbonate sand increases, the total impulse increases (Figures 7a and 8), as is expected based on historic work [7]. It can also be seen that the carbonate sands at all moisture contents result in a similar loading to the comparable quartz sand tests. This is contrary to what would be expected for a sand with lower bulk density, indicating that

bulk density may be of a lower priority in governing blast events than previous models have predicted.

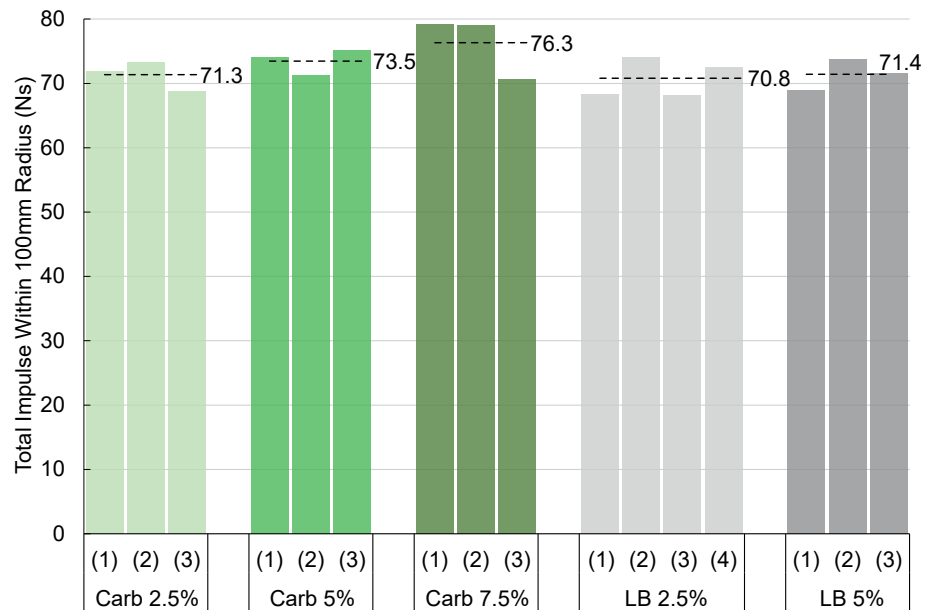


**Figure 8.** Total interpolated impulse within the 100 mm instrumented region for each test, with the average for each series overlaid as a dashed line.

#### 4. Discussion and Conclusions

Table 4 summarises both the experimental results, and the output from the empirical models. This shows that, relative to the 2.5% moisture content quartz sand, carbonate sand is predicted to produce lower loading due to the lower bulk density. In contrast, the experimental results show an increase over the quartz sand baseline. Combining the measured increase and the predicted decrease, this indicates that a balance of factors affecting the loading is incorrect in previous models [2,7]. In the case of carbonate sand at 7.5% moisture content, this additional factor accounts for an 11.6% increase over what is predicted from previous work [7], indicating that there is an overdependence on the role of bulk density in previous models. This assumption is supported by work on explosives buried in materials other than soils [17,34], where charges submerged in water showed no decrease in impulse, nor did those within saturated lead shot [34], where again, despite the increased bulk density, the measured impulse was comparable with that in saturated sand.

**Table 4.** Difference in measured and predicted total impulse relative to the 2.5% LB series.

Series	Measured	Westine Prediction	Imod Prediction
LB 2.5%	Baseline	Baseline	Baseline
LB 5.0%	0.8%	1.1%	9.31%
Carb 2.5%	0.7%	−12.2%	−8.4%
Carb 5.0%	3.8%	−12.0%	−6.6%
Carb 7.5%	7.8%	−10.6%	−3.7%

Particle mineralogy and, hence, the role of particle breakage have not previously been investigated. The low degree of breakage seen can be explained to a certain degree by Xiao et al. [13], who found that the extent of particle breakage was higher under quasi-static loading than under dynamic loading conditions at the same stress. The quartz-based sands in this paper were more friable than the similarly sized carbonate sands, which is in contrast to the published literature but is possibly a product of the artificial nature of the sand tested and that the quartz sand was more uniform [15]. However, the results suggest that the

reduction in particle breakage could have an impact on the overall impulse delivered to the target, with the lower degree of particle breakage in the carbonate sands correlating with the increase in impulse over the quartz sands. However, this is very much a second-order process due to the small variations observed. The dynamic compaction response of the two sands could also be a cause for variations in impulse. Testing by Weckert and Resnyansky [35] has shown that, in dynamic testing, the stiffness of the carbonate sand is lower than that of the quartz sands and that this is also a product of the moisture content of the sand, as seen previously [36]. It is known that the plate-like particles of carbonate sands likely produce soils with greater shear strength at low stresses [15,16]. At higher stresses, the authors of [35] indicated little difference between the two soils at higher degrees of compression. Whether this behaviour has an impact at the high stresses seen in blast events is as yet unknown but will be the focus of future research.

To conclude, this work has found the following:

- There is no substantial difference in the total impulse and specific impulse distribution between charges buried in quartz and carbonate sand;
- There is no increase in the observed particle breakage for carbonate sand over quartz sand during buried charge testing. Moreover, there is a small observed increase in breakage of quartz sand over carbonate sand.

**Author Contributions:** Conceptualisation, T.L. and S.C.; methodology, T.L. and S.C.; formal analysis, T.L. and R.W.; writing—original draft preparation, T.L.; writing—review and editing, S.C., R.W., S.R., M.G. and I.E.; supervision, S.C. and S.R.; experimental management, T.L.; funding acquisition, M.G. and I.E. All authors have read and agreed to the published version of the manuscript.

**Funding:** This research was funded by a Defence Science and Technology Laboratory (Dstl) funded EPSRC CASE studentship. The experimental work, including historical data, was funded by Dstl under contract DSTLX-1000059883.

**Data Availability Statement:** The data presented in this study are available from the corresponding author upon request.

**Acknowledgments:** The authors recognise the work of the technical support staff at Blastech Ltd. without whom we would have never been able to have such excellent datasets to work with.

**Conflicts of Interest:** The authors declare no conflict of interest.

## Abbreviations

The following abbreviations are used in this manuscript:

CoBL	Characterisation of Blast Loading testing apparatus
Dstl	Defence Science and Technology Laboratory
LB	Leighton Buzzard—a type of quartz sand
PSD	Particle Size Distribution

## References

1. United Nations. *Assistance in Mine Action, Report of the Secretary-General*; OCHA: New York, NY, USA, 2021; Volume 11018.
2. Westine, P.S.; Morris, B.L.; Cox, P.A.; Polch, E.Z. *Development of Computer Program for Floor Plate Response from Land Mine Explosions*; Technical Report; Southwest Research Institute: San Antonio, TX, USA, 1985.
3. Ehr Gott, J.Q.; Akers, S.A.; Windham, J.E.; Rickman, D.D.; Danielson, K.T. The influence of soil parameters on the impulse and airblast overpressure loading above surface-laid and shallow-buried explosives. *Shock Vib.* **2011**, *18*, 857–874. [[CrossRef](#)]
4. Hlady, S. Effect of Soil Parameters on Land Mine Blast. In Proceedings of the 18th International Symposium on Military Aspects of Blast and Shock, Bad Reichenhall, Germany, 27 September–1 October 2004.
5. Grujicic, M.; Pandurangan, B.; Huang, Y.; Cheeseman, B.A.; Roy, W.N.; Skaggs, R.R. Impulse loading resulting from shallow buried explosives in water-saturated sand. *Proc. Inst. Mech. Eng. Part L J. Mater. Des. Appl.* **2007**, *221*, 21–35. [[CrossRef](#)]
6. Anderson, C.E.; Behner, T.; Weiss, C.E.; Bigger, R.; Chocron, S. *Mine Blast Loading: Experiments and Simulations*; Technical Report; Southwest Research Institute: San Antonio, TX, USA, 2009.
7. Clarke, S.D.; Fay, S.D.; Warren, J.A.; Tyas, A.; Rigby, S.E.; Reay, J.J.; Livesey, R.; Elgy, I. Predicting the role of geotechnical parameters on the output from shallow buried explosives. *Int. J. Impact Eng.* **2017**, *102*, 117–128. [[CrossRef](#)]

8. Denefeld, V.; Heider, N.; Holzwarth, A. Measurement of the spatial specific impulse distribution due to buried high explosive charge detonation. *Def. Technol.* **2017**, *13*, 219–227. [[CrossRef](#)]
9. Fox, D.M.; Akers, S.A.; Leiste, U.H.; Fournery, W.L.; Windham, J.E.; Lee, J.S.; Ehr Gott, J.Q.; Taylor, L.C. The effects of air filled voids and water content on the momentum transferred from a shallow buried explosive to a rigid target. *Int. J. Impact Eng.* **2014**, *69*, 182–193. [[CrossRef](#)]
10. Leiste, U. The effect of air filled voids on impulse delivered by a buried mine. *Fragblast* **2018**, *7*, 31.
11. Clarke, S.D.; Fay, S.D.; Warren, J.A.; Tyas, A.; Rigby, S.E.; Reay, J.J.; Livesey, R.; Elgy, I. Geotechnical causes for variations in output measured from shallow buried charges. *Int. J. Impact Eng.* **2015**, *86*, 274–283. [[CrossRef](#)]
12. Heider, N.; Denefeld, V.; Aurich, H. Analysis of global momentum transfer due to buried mine detonation. *Def. Technol.* **2019**, *15*, 821–827. [[CrossRef](#)]
13. Xiao, Y.; Yuan, Z.; Chu, J.; Liu, H.; Huang, J.; Luo, S.N.; Wang, S.; Lin, J. Particle breakage and energy dissipation of carbonate sands under quasi-static and dynamic compression. *Acta Geotech.* **2019**, *14*, 1741–1755. [[CrossRef](#)]
14. Rasouli, M.R.; Hassanlourad, M. Comparative Study of Carbonate and Quartz Sand Based on Energy Concepts. *Amirkabir J. Civ. Eng.* **2017**, *49*, 29–31. [[CrossRef](#)]
15. Coop, M.R.; Sorensen, K.K.; Freitas, T.B.; Georgoutsos, G. Particle breakage during shearing of a carbonate sand. *Geotechnique* **2004**, *54*, 157–163. [[CrossRef](#)]
16. Golightly, C.R. The Engineering Properties of Carbonate Sands. Ph.D. Thesis, University of Bradford, Bradford, UK, 1988.
17. Clarke, S.; Rigby, S.; Fay, S.; Barr, A.; Tyas, A.; Gant, M.; Elgy, I. Characterisation of Buried Blast Loading. *Proc. R. Soc. A* **2020**, *476*, 20190791. [[CrossRef](#)] [[PubMed](#)]
18. Hardin, B.O. Crushing of soil particles. *J. Geotech. Eng.* **1985**, *111*, 1177–1192. [[CrossRef](#)]
19. Einav, I. Breakage mechanics—Part I: Theory. *J. Mech. Phys. Solids* **2007**, *55*, 1274–1297. [[CrossRef](#)]
20. McDowell, G.; Bolton, M.; Robertson, D. The fractal crushing of granular materials. *J. Mech. Phys. Solids* **1996**, *44*, 2079–2101. [[CrossRef](#)]
21. Yu, F. Particle breakage in granular soils: A review. *Part. Sci. Technol.* **2021**, *39*, 91–100. [[CrossRef](#)]
22. Yang, J.; Luo, X. Exploring the relationship between critical state and particle shape for granular materials. *J. Mech. Phys. Solids* **2015**, *84*, 196–213. [[CrossRef](#)]
23. Cho, G.; Dodds, J.; Santamarina, J. Particle Shape Effects on Packing Density, Stiffness, and Strength: Natural and Crushed Sands. *J. Geotech. Geoenviron. Eng.* **2006**, *132*, 591–602. [[CrossRef](#)]
24. Ghafghazi, M.; Shuttle, D.; DeJong, J. Particle breakage and the critical state of sand. *Soils Found.* **2014**, *54*, 451–461. [[CrossRef](#)]
25. Clarke, S.D.; Fay, S.D.; Warren, J.A.; Tyas, A.; Rigby, S.E.; Elgy, I. A large scale experimental approach to the measurement of spatially and temporally localised loading from the detonation of shallow-buried explosives. *Meas. Sci. Technol.* **2015**, *26*, 015001. [[CrossRef](#)]
26. Rigby, S.E.; Tyas, A.; Clarke, S.D.; Fay, S.D.; Reay, J.J.; Warren, J.A.; Gant, M.; Elgy, I. Observations from preliminary experiments on spatial and temporal pressure measurements from near-field free air explosions. *Int. J. Prot. Struct.* **2015**, *6*, 175–190. [[CrossRef](#)]
27. Clarke, S.D.; Fay, S.D.; Rigby, S.E.; Tyas, A.; Warren, J.A.; Reay, J.J.; Fuller, B.J.; Gant, M.T.; Elgy, I.D. Blast quantification using hopkinson pressure bars. *J. Vis. Exp.* **2016**, *2016*, 53412. [[CrossRef](#)]
28. Tyas, A.; Warren, J.; Bennett, T.; Fay, S. Prediction of clearing effects in far-field blast loading of finite targets. *Shock Waves* **2011**, *21*, 111–119. [[CrossRef](#)]
29. Fay, S.D.; Clarke, S.D.; Tyas, A.; Warren, J.; Rigby, S.; Bennett, T.; Elgy, I.; Gant, M. Measuring the Spatial and Temporal Pressure Variation from Buried Charges. In Proceedings of the 23rd International Symposium of Military Aspects of Blast and Shock, Oxford, UK, 8–12 September 2014.
30. Clarke, S.; Fay, S.; Tyas, A. Repeatability of buried charge testing. In Proceedings of the 23rd International Symposium on Military Aspects of Blast and Shock, Oxford, UK, 8–12 September 2014.
31. NATO. AEP-55, Procedures for Evaluation the Protection Level of Logistic and Light Armoured Vehicles: Vol 2 Mine Threat. *Allied Eng. Publ.* **2014**, *2*, 12.
32. Rigby, S.E.; Knighton, R.; Clarke, S.D.; Tyas, A. Reflected Near-field Blast Pressure Measurements Using High Speed Video. *Exp. Mech.* **2020**, *60*, 875–888. [[CrossRef](#)]
33. Taylor, L.C.; Fournery, W.L.; Leiste, U. Loading Mechanisms from Shallow Buried Explosives. In Proceedings of the 24th International Symposium on Ballistics, New Orleans, LA, USA, 22–26 September 2008.
34. Fournery, W.; Leiste, U.; Bonenberger, R.; Goodings, D. Mechanism of loading on plates due to explosive detonation. *Fragblast* **2005**, *9*, 205–217. [[CrossRef](#)]
35. Weckert, S.A.; Resnyansky, A.D. Experiments and modelling for characterisation and validation of a two-phase constitutive model for describing sands under explosive loading. *Int. J. Impact Eng.* **2022**, *166*, 104234. [[CrossRef](#)]
36. Barr, A.D.; Clarke, S.D.; Petkovski, M.; Tyas, A.; Rigby, S.E.; Warren, J.; Kerr, S. Effects of strain rate and moisture content on the behaviour of sand under one-dimensional compression. *Exp. Mech.* **2016**, *56*, 1625–1639. [[CrossRef](#)]

**Disclaimer/Publisher's Note:** The statements, opinions and data contained in all publications are solely those of the individual author(s) and contributor(s) and not of MDPI and/or the editor(s). MDPI and/or the editor(s) disclaim responsibility for any injury to people or property resulting from any ideas, methods, instructions or products referred to in the content.